# A SIMPLE MODEL FOR THE EVALUATION OF FATIGUE DEGRADATION LAWS FOR INTERFACE ELEMENTS

**Carlos A. López-Armas\*, Ugo Galvanetto\* and Paul Robinson\***
**\*Department of Aeronautics, Imperial College, London, U.K.**

**Keywords**: *fatigue; delamination; interface elements*

*Abstract*

*A simple model that represents interface elements subjected to fatigue loading is proposed and used to evaluate three different constitutive laws as well as three different damage definitions. The three constitutive laws are bilinear, third-order polynomial and linear-polynomial while the damage definitions are based on the degradation of stiffness and the energy consumed.*

*The behaviour of the constitutive laws and damage formulations has been found to be similar but with some variations in their sensitivity to the size of the elements and to the number of cycles applied in each load step. The results confirm that the more accurate results are found for smaller values of these two variables.*

## 1 Introduction

Because of their high strength-to-weight ratios the use of laminated composite materials in airframes, for both civil and military aircraft, has become more extensive in the last few years and this is a trend that will continue in the foreseeable future.

One of the most important failure mechanisms of composite materials is delamination. This can occur due to manufacturing defects, impacts on the surface, edge effects, fatigue loading, etc. This type of failure can make a component lose its strength and/or stiffness and eventually lead to failure.

The conditions under which some aircraft components operate, such as the blades of a helicopter, are known to cause composites to fail due to fatigue loading. Since failure of these components can result in catastrophe it is very important to be able to predict life spans.

This can be achieved either by experimentation or by doing computer simulations. Because experimentation tends to be a lengthy and expensive process, in recent years a lot of emphasis has been placed on computer simulation. [1-4]

One of the methods that have been proposed for predicting delamination is using Finite Element Analysis (FEA) with interface elements located between adjacent layers of the composites being modelled. The interface element is defined as a zero-thickness medium that ensures stress and displacement transfers from one composite ply to another. An interface constitutive law is required to establish the behaviour of the element. [5]

The simulation of fatigue-driven delamination in laminated composites is a relatively new field of research. One approach is to use interface elements that have constitutive laws that allow fatigue degradation to occur. [6-8]

Since the FEA of fatigue-induced delamination can be relatively costly in terms of time and computing power a very simple model is proposed as a way to quickly evaluate and develop different interface element constitutive laws and fatigue damage formulations.

## 2 Implementation

### 2.1 Model description

The model, shown in Figure 1, resembles a ply of laminated composite attached to a fixed surface by means of springs, which act as interface elements, located at constant intervals ($\Delta l$). This ply, of width $W$, is attached along one of its edges to a cylinder of radius ($R$) to which a certain moment ($M_a$) is applied. The applied moment makes the cylinder rotate and the springs are degraded accordingly. The springs are fixed to the 'ground' and their connection with the cylinder is constrained in such a way that the springs are always vertical independently of the rotation of the cylinder. When a spring has completely degraded it can be said that delamination growth has occurred. The behaviour

of the degradation of the springs is ruled by the interface constitutive law being used.

The critical moment ($M_c$) is defined as the moment required to degrade completely the first spring and if the moment applied is kept constant then this critical moment is enough to break all springs. If we equate the work done by the critical moment over the change in rotation ($\Delta\theta$) to the energy consumed as the crack advances through the area defined by $\Delta\theta R \cdot W$ at an interface with a critical energy release rate ($G_c$) we have

$$M_c \Delta\theta = G_c \Delta\theta RW \qquad (1)$$

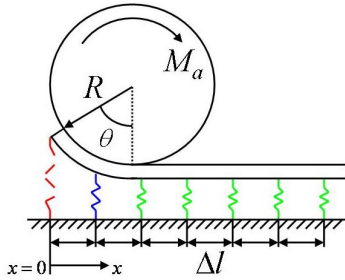which can be rewritten as

$$M_c = G_c RW \qquad (2)$$


Fig. 1. Model representation.

In Figure 2 a typical static response of the model is shown and it can be seen how as the applied moment is increased the rotation of the cylinder is increased too until a critical angle ($\alpha$) is reached at which the applied moment becomes critical and cannot be increased any more.
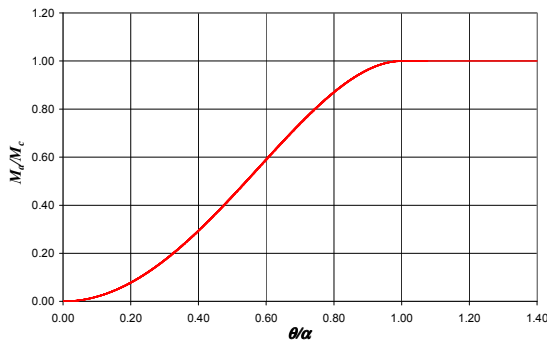

Fig. 2 Typical static response of the model

The critical angle ($\alpha$), at which the first spring fails, is related to the maximum relative displacement of a spring when it fails ($\delta_c$) and is given by

$$\alpha = \cos^{-1}\left(\frac{R - \delta_c}{R}\right) \qquad (3)$$

If a moment $M_a$ is applied to the cylinder such that

$$M_a < M_c \qquad (4)$$

the cylinder will rotate from the origin a given amount $\theta < \alpha$.

In Figure 3 it can be seen that the angle ($\omega_i$) and the displacement ($\delta_i$) for any spring at any given rotation ($\theta$) can be obtained from

$$\omega_i = \sin^{-1}\left(\frac{\theta R - x_i}{R}\right) \qquad (5)$$

$$\delta_i = R(1 - \cos\omega_i) \qquad (6)$$

where $x_i$ is the distance from the initial position of the cylinder to the location of the spring.
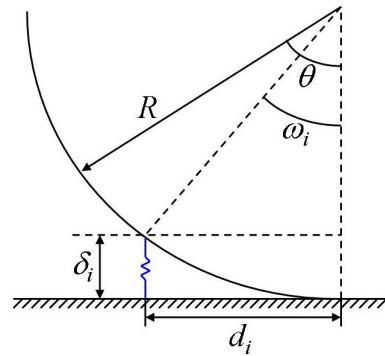

Fig. 3. Angle, displacement and distance of a spring

Once the displacement is known, the stress of the spring ($\sigma_i$) can be obtained by using any of the interface constitutive laws. Then the reaction force in the spring ($F_i$) will be

$$F_i = \sigma_i \Delta l W \qquad (7)$$

and the distance and the moment generated by the spring ($M_i$) are computed using

$$d_i = \theta R - x_i \qquad (8)$$

$$M_i = F_i d_i \qquad (9)$$

The total moment ($M_t$) can be obtained by adding all the active springs

$$M_t = \sum_{1}^{n} M_i \qquad (10)$$

and by comparing it with the desired applied moment ($M_a$) it can be determined if the rotation applied ($\theta$) is the correct one and if not modify it and recalculate everything again.

Once that static equilibrium has been reached the fatigue loading procedure begins and it follows the same strategy described above, the only

difference being the change in the damage formulation which is now the combination of two terms the static and the fatigue one.
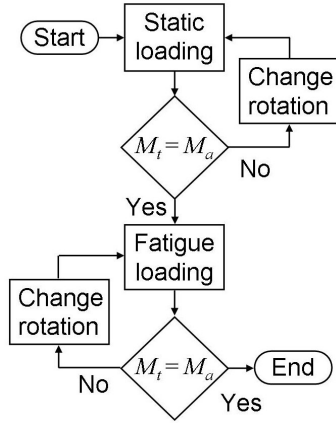


Fig. 4 Flow chart.

## 2.2 Interface static load constitutive laws

Three different interface constitutive laws were implemented in the model: bilinear, third-order polynomial and linear-polynomial. The same values were used for all computations and are shown in Table 1.

### 2.2.1 Bilinear law

The bilinear constitutive law for interface elements proposed by Alfano and Crisfield [6], shown in Figure 5, was initially used to define the properties of the springs in the simple cylinder model.
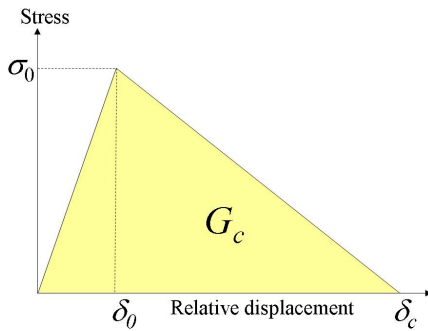


Fig. 5. Bilinear interface law

In the bilinear law when a relative displacement ($\delta$) below the elastic limit ($\delta_0$) is applied a linear-elastic behaviour occurs:

$$\sigma = K\delta \qquad \text{if } \delta \leq \delta_0 \qquad (11)$$

where the high penalty stiffness ($K$), used to approximate the state of the interface for which a non-zero stress corresponds to a zero relative displacement, is defined as

$$K = \frac{\sigma_0}{\delta_0} \qquad (12)$$

When the elastic limit value is reached, corresponding to the maximum stress value ($\sigma_0$), the interface element starts to be damaged or degraded until it reaches a critical displacement value ($\delta_c$). This damage value ($D$) effectively reduces the stiffness:

$$\sigma = (1 - D)K\delta \qquad \text{if } \delta_0 < \delta < \delta_c \quad (13)$$

where the damage is given by

$$D = \left(\frac{\delta - \delta_0}{\delta}\right)\left(\frac{\delta_c}{\delta_c - \delta_0}\right) \qquad \text{if } \delta_0 < \delta < \delta_c \quad (14)$$

and finally the element fails when $\delta$ reaches or exceeds $\delta_c$:

$$\sigma = 0 \qquad \text{if } \delta_c \leq \delta \qquad (15)$$

In Figure 5 we can see how the $\delta$ and $\sigma$ can be related in a non-linear fashion for Mode I (opening). The area under the curve represents the critical energy release rate ($G_c$) for Mode I and its value is given by

$$G_c = \frac{\delta_c \sigma_0}{2} \qquad (16)$$

| | | |
|---|---|---|
| $\delta_0$ | $1.00 \times 10^{-6}$ | mm |
| $\sigma_0$ | 30 | N/mm$^2$ |
| $G_c$ | 0.260 | N/mm |
| $\Delta l$ | $1.00 \times 10^{-2}$ | mm |
| $R$ | 100 | mm |
| $W$ | 1 | mm |

Table 1. Values used in the computations.

### 2.2.2 Third order polynomial law

This interface constitutive law, proposed by Tvergaard [9] and adapted by Pinho et al. [10] to interface elements, is characterised for not having any discontinuities as opposed to the previous one and that the slope at the failure of the interface element is zero. As the name implies the shape of this interface constitutive law is a curve given by the following third-order polynomial function:

$$\sigma = \frac{27}{4}\sigma_0\left(1 - \frac{\delta}{\delta_c}\right)^2 \frac{\delta}{\delta_c} \qquad \text{if } \delta \leq \delta_c \qquad (17)$$

where the value of $\sigma_0$ corresponds to a value of
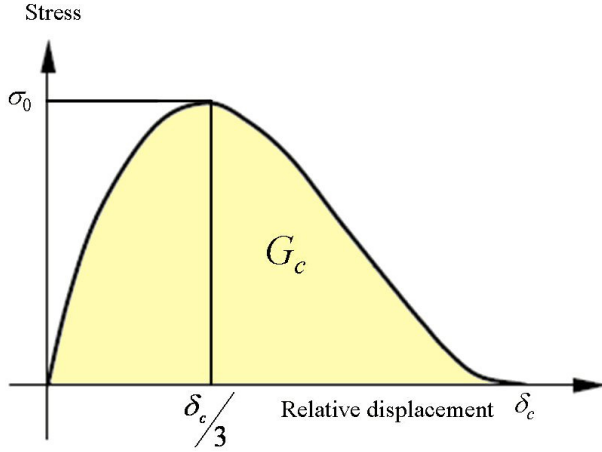
$$\delta = \frac{\delta_c}{3} \qquad (18)$$



Fig. 6. Third order polynomial law

In order to express Equation 17 in the same form as Equation 13 the damage (*D*) is defined as

$$D = 2\frac{\delta}{\delta_c} - \left(\frac{\delta}{\delta_c}\right)^2 \qquad \text{if } \delta \leq \delta_c \qquad (19)$$

and the stiffness (K) is found to be

$$K = \frac{27}{4}\frac{\sigma_0}{\delta_c} \qquad \text{if } \delta \leq \delta_c \qquad (20)$$

The critical energy release rate is also given by the area under the curve, as shown in Figure 6, and its value corresponds to

$$G_c = \frac{27}{48}\delta_c\sigma_0 \qquad (21)$$

*2.2.3 Linear-polynomial law*

This law, proposed by Pinho et al. [10], can be defined as a combination of the two previous ones.

It is similar to the bilinear interface constitutive law in the linear-elastic behaviour before damage initiation and it is similar to the third –order polynomial one in the zero slope value both at the initiation of damage and at the failure of the interface element by using a high-order damage variable. It is given by

$$\sigma = \left[1 + \left(\frac{\delta - \delta_0}{\delta_c - \delta_0}\right)^2\left(2\frac{\delta - \delta_0}{\delta_c - \delta_0} - 3\right)\right]K\delta_0 \qquad (22)$$

for values of $\delta$ between $\delta_0$ and $\delta_c$.



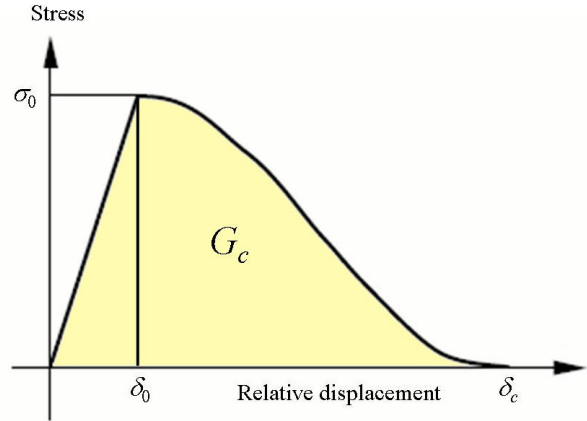Fig. 7. Linear-polynomial law

If, again, this law is expressed in the same form as Equation 13 then the damage (*D*) for values of $\delta$ between $\delta_0$ and $\delta_c$ is given by

$$D = 1 - \frac{\delta_0}{\delta}\left[1 + \left(\frac{\delta - \delta_0}{\delta_c - \delta_0}\right)^2\left(2\frac{\delta - \delta_0}{\delta_c - \delta_0} - 3\right)\right] \qquad (23)$$

and the value of *Gc* is given by Equation 16.

**2.3 Alternative static damage formulations**

The static damage formulations of the interface constitutive laws that have been discussed are all based on the degradation of the stiffness of the element.

Two additional different static damage formulations were proposed and investigated for the bilinear interface constitutive law.

*2.3.1 First energy based static damage formulation*

An alternative bilinear constitutive law has been proposed in which damage is now a function of the area covered by the triangle generated by connecting the origin, $\delta_0,\sigma_0$ and $\delta,\sigma$ as it can be seen in Figure 8. This area will have a value of zero, and thus no damage, for values of $\delta$ lower that $\delta_0$ and will increase linearly as $\delta$ increases until it reaches $\delta_c$. Damage (*D*) is defined as the ratio between the 'used' area, as shown in Figure 8, and the total area (*Gc*) and is given by the following relationship:

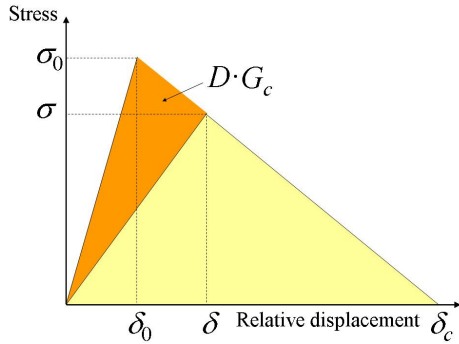$$D = \frac{\delta - \delta_0}{\delta_c - \delta_0} \qquad \text{if } \delta_0 < \delta < \delta_c \qquad (24)$$

Fig. 8. First energy based damage formulation

Since the growth of damage is a linear function of $\delta$, the interface constitutive law can be reformulated as

$$\sigma = (1-D)\sigma_0 \qquad \text{if } \delta_0 < \delta < \delta_c \qquad (25)$$

*2.3.2 Second energy based static damage formulation*

A different damage formulation can be proposed where the damage ($D$) is a function that mirrors the behaviour of the energy consumed during static delamination. This is done by comparing the dark area with the total area, as shown in Figure 9.
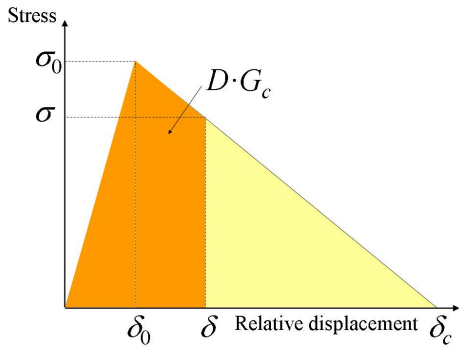

Fig. 9. Energy based damage formulation

The damage ($D$) is now defined as

$$D = 1 - \left(\frac{\delta_c - \delta}{\delta_c}\right)\left(\frac{\delta_c - \delta}{\delta_c - \delta_0}\right) \text{ if } \delta_0 < \delta < \delta_c \quad (26)$$

and the interface constitutive law can be rewritten as

$$\sigma = (1-D)\sigma_0\left(\frac{\delta_c}{\delta_c - \delta}\right) \qquad \text{if } \delta_0 < \delta < \delta_c \quad (27)$$

## 3 Fatigue damage formulations

The scheme for introducing fatigue damage into the interface element being investigated is based on an exponential law (Peerlings) [11] which has been used with success by Robinson et al. [7] and Muñoz et al. [8] for fatigue degradation of bilinear interface elements.

### 3.1 Fatigue damage formulations based on an exponential law

In order to combine the stress/relative displacement relationship of the previous section with a fatigue model, the rate of damage ($\partial D/\partial t$) is split into the sum of its static and fatigue components:

$$\frac{\partial D}{\partial t} = \frac{\partial D_s}{\partial t} + \frac{\partial D_f}{\partial t} \qquad (28)$$

The static component is defined depending on the interface constitutive law and the damage formulation used to compute it, while the fatigue component is defined by using an exponential law.

*3.1.1 Stiffness based fatigue damage formulation for the bilinear law*

Rearranging Equation 4

$$D_s = \frac{\delta_c}{\delta_c - \delta_0} - \frac{\delta_0 \delta_c}{\delta_c - \delta_0}\frac{1}{\delta} \qquad (29)$$

and by differentiating Equation (29) with respect to time the static component is found

$$\frac{\partial D_s}{\partial t} = \frac{\delta_0 \delta_c}{\delta_c - \delta_0}\frac{1}{\delta^2}\frac{\partial \delta}{\partial t} \qquad \text{for } \frac{\partial \delta}{\partial t} \geq 0 \quad (30)$$

By integrating Equation (30) over a certain number of loading cycles ($\Delta N$) the rate of damage on a cycle based formulation is obtained

$$\int_{t(N)}^{t(N+\Delta N)}\frac{\partial D_s}{\partial t}\,dt = \int_{t(N)}^{t(N+\Delta N)}\frac{\delta_0 \delta_c}{\delta_c - \delta_0}\frac{1}{\delta^2}\frac{\partial \delta}{\partial t}\,dt \qquad (31)$$

where $t(N)$ is the time corresponding to the end of cycle $N$ and $t(N+\Delta N)$ is the time corresponding to the end of cycle $N+\Delta N$, which yields

$$D_s\Big|_N^{N+\Delta N} = \frac{\delta_0 \delta_c}{\delta_c - \delta_0}\left(-\frac{1}{\delta}\right)\Big|_N^{N+\Delta N} \qquad (32)$$

$$D_{s\,N+\Delta N} - D_{s\,N} = \frac{\delta_0 \delta_c}{\delta_c - \delta_0}\left(\frac{1}{\delta_N} - \frac{1}{\delta_{N+\Delta N}}\right) \qquad (33)$$

The exponential law used to find the fatigue component of the rate of damage is a modified version of Peerlings' law [7] and is given by

$$D_f = \frac{\partial D_f}{\partial t} = C e^{\lambda D} \left( \frac{\delta}{\delta_a} \right) \quad (34)$$

where $\delta_a$ is a displacement quantity introduced for dimensional reasons and $\beta$, $\lambda$ and $C$ are parameters whose values are determined by studying the influence of their variation.

Peerlings' law allows the damage to grow with the number of cycles even if the initial damage at the interface is zero.

If Equation (34) is rearranged and integrated over one cycle

$$e^{-\lambda D} \frac{\partial D_f}{\partial t} = C \left( \frac{\delta}{\delta_a} \right)^\beta \frac{\dot{\delta}(t)}{\delta_a} \quad (35)$$

$$\int_{t(N)}^{t(N+1)} e^{-\lambda D} \frac{\partial D_f}{\partial t} dt = \int_{t(N)}^{t(N+1)} C \left( \frac{\delta}{\delta_a} \right)^\beta \frac{\dot{\delta}(t)}{\delta_a} dt \quad (36)$$

$$\int_{D(N)}^{D(N+1)} e^{-\lambda D} dD = \frac{C}{\delta_a^{\beta+1}} \int_{\delta(N)}^{\delta(N+1)} \delta^\beta d\delta \quad (37)$$

In Equations (36) and (37) only the fatigue component of the damage is assumed to vary and therefore $dD_f = dD$. If the derivative $\partial D_f / \partial N$ does not change rapidly with increasing cycles, as is usual for high cycle fatigue, then it can be written

$$D_f(N + \Delta N) \cong D_f(N) + \frac{\partial D_f}{\partial N} \Delta N \quad (38)$$

and therefore for $\Delta N = 1$

$$e^{-\lambda D_f(N+1)} \cong e^{-\lambda D_f(N)} \left( 1 - \lambda \frac{\partial D_f}{\partial N} \right) \quad (39)$$

Because the fatigue law is valid only if the rate of damage is larger or equal to zero, it is possible to find the formal equation for the rate of damage due to the fatigue phenomenon

$$\frac{\partial D_f}{\partial N} = \frac{C}{1+\beta} e^{\lambda D} \left[ \left( \frac{\delta_{max}}{\delta_a} \right)^{1+\beta} - \left( \frac{\delta_{min}}{\delta_a} \right)^{1+\beta} \right] \quad (40)$$

where $\delta_{max}$ is the maximum value of the displacement component $\delta$ during the cycle and $\delta_{min}$ the corresponding minimum value.

In the present formulation the value of $\delta_a$ was chosen as the value of the relative displacement at failure ($\delta_c$). The value of $\delta_c$ depends on the critical energy release rate and the maximum stress defined for the interface element in the numerical model.

Assuming for simplicity that $\delta_{min}$ is zero and that $\delta_{max}$ is $\delta$, Equation (40) can be rewritten as

$$\frac{\partial D_f}{\partial N} = \frac{C}{1+\beta} e^{\lambda D} \left( \frac{\delta}{\delta_c} \right)^{1+\beta} \quad (41)$$

Following Equation (28), by adding Equations (33) and (41) the damage rate is found to be

$$\frac{\partial D}{\partial N} = \frac{\delta_0 \delta_c}{\delta_c - \delta_0} \frac{1}{\delta^2} \frac{\partial \delta}{\partial N} + \frac{C}{1+\beta} e^{\lambda D} \left( \frac{\delta}{\delta_c} \right)^{1+\beta} \quad (42)$$

and therefore

$$D(N + \Delta N) = D(N) + \int_N^{N+\Delta N} \frac{\partial D}{\partial N} dN \quad (43)$$

and defining the fatigue component as a function $G(D, \delta)$

$$D(N + \Delta N) = D(N) + \int_N^{N+\Delta N} \left( \frac{\delta_0 \delta_c}{\delta_c - \delta_0} \frac{1}{\delta^2} \frac{\partial \delta}{\partial N} + G(D, \delta) \right) dN$$

for $\delta_{N+\Delta N} \geq \delta_N$ $\quad (44)$

The integration of the static damage term in Equation (44) is given by Equation (33). The integration of the fatigue damage component can be accomplished observing that, for the continuity of $D$, there is a real number m, with $0 \leq \mu \leq 1$, such that

$$\int_N^{N+\Delta N} G(D, \delta) dN = \Delta N G(D_\mu, \delta_\mu) \quad (46)$$

where $D_\mu$ and $\delta_\mu$ are given by

$$D_\mu = (1 - \mu) D(N) + \mu D(N + \Delta N) \quad (47)$$

$$\delta_\mu = (1 - \mu) \delta(N) + \mu \delta(N + \Delta N) \quad (48)$$

In all the computations that have been done the value of $\mu = 0.7$ has been taken from [7] giving satisfactory results, but the problem of finding an optimal value of $\mu$ is not trivial.

The damage growth rate is given by

$$D_{N+\Delta N} = D_N + \underbrace{\frac{\delta_0 \delta_c}{\delta_c - \delta_0}\left(\frac{1}{\delta_N} - \frac{1}{\delta_{N+\Delta N}}\right)}_{static} + \underbrace{\Delta N \frac{C}{1+\beta} e^{\lambda D_\mu}\left(\frac{\delta_\mu}{\delta_c}\right)^{1+\beta}}_{fatigue}$$

for $\delta_{N+\Delta N} \geq \delta_N$ \hfill (48)

and since the damage variable appears on both sides of Equation (48) its value must be determined iteratively. It can be rewritten as

$$H = D_{N+\Delta N} - D_N - \underbrace{\frac{\delta_0 \delta_c}{\delta_c - \delta_0}\left(\frac{1}{\delta_N} - \frac{1}{\delta_{N+\Delta N}}\right)}_{static} - \underbrace{\Delta N \frac{C}{1+\beta} e^{\lambda D_\mu}\left(\frac{\delta_\mu}{\delta_c}\right)^{1+\beta}}_{fatigue} = 0$$

\hfill (49)

The residual function is defined as

$$H = H\big(D(N + \Delta N), \delta(N + \Delta N)\big) \qquad (50)$$

so that the new value of damage ($D$) can be found by applying the standard Newton-Raphson method to Equation 50. It is mentioned in [7] that the success of the iterative procedure depends on the values of the parameters defining the damage due to fatigue: $\beta$, $\lambda$ and $C$. A fixed value of $\lambda = 0.5$ was adopted for all of the cases analysed [7]. The values of $\beta$ and $C$ used in the computations are shown in Table 2.

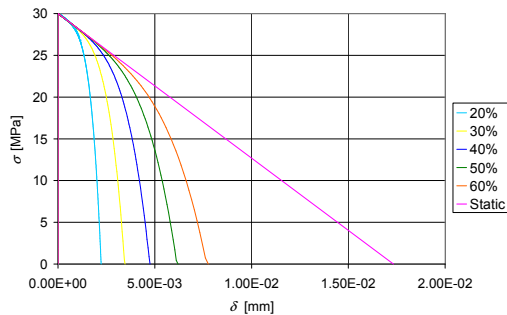| | $\beta$ | $C$ |
|---|---|---|
| Bilinear law, stiffness | 2.0 | $2 \times 10^{-6}$ |
| Polynomial law, stiffness | 5.5 | $2.94 \times 10^{-1}$ |
| Bilinear law, area | 2.9 | $6.35 \times 10^{-2}$ |
| Bilinear law, energy | 2.65 | $2.78 \times 10^{-2}$ |

Table 2. Coefficient values for different schemes



Fig. 10. Fatigue behaviour of springs

The typical response of a bilinear interface element under fatigue loading is shown in Figure 10, where the key indicates the applied cyclic moment as a percentage of the static maximum moment to cause delamination growth.

*3.1.2 Stiffness based fatigue damage formulation for the polynomial law*

After finding the different fatigue damage formulations for the bilinear law, the same is done to the polynomial law by following the procedure uses in section *3.1.1* and the static component is

$$D_{s\,N+\Delta N} - D_{s\,N} = \frac{2}{\delta_c}\left(\delta_{N+\Delta N} - \delta_N - \frac{\delta^2_{N+\Delta N}}{2\delta_c} + \frac{\delta^2_N}{2\delta_c}\right)$$

for $\delta_{N+\Delta N} \geq \delta_N$ \hfill (51)

to be substituted in Equation (49).

*3.1.3 First energy based fatigue damage formulation for the bilinear law*

Following the same procedure the static component of the damage growth rate is found to be

$$D_{s\,N+\Delta N} - D_{s\,N} = \frac{\delta_{N+\Delta N}}{\delta_c - \delta_0} - \frac{\delta_N}{\delta_c - \delta_0}$$

for $\delta_{N+\Delta N} \geq \delta_N$ \hfill (52)

which is substituted in Equation (49).

*3.1.4 Second energy based fatigue damage formulation for the bilinear law*

Again, the same procedure is followed and the static component for this damage formulation is given by

$$D_{s\,N+\Delta N} - D_{s\,N} = \left(\frac{2\delta_{N+\Delta N}}{\delta_c - \delta_0} - \frac{2\delta^2_{N+\Delta N}}{\delta_c(\delta_c - \delta_0)}\right) - \left(\frac{2\delta_N}{\delta_c - \delta_0} - \frac{\delta^2_N}{\delta_c(\delta_c - \delta_0)}\right)$$

for $\delta_{N+\Delta N} \geq \delta_N$ \hfill (53)

for its substitution in Equation (49).

## 4 Results

The model has been used to investigate the effectiveness of the methods proposed to introduce fatigue damage in interface elements. The sensitivity of the predicted response has been examined for a number of parameters including coefficients in the damage formulations themselves, the spacing of the spring elements ($\Delta l$) and the number of cycles applied for each load step ($\Delta N$).

### 4.1 Comparison with experimental results

Figure 10 shows that the bilinear interface element with fatigue damage according to Peerlings' Law can reproduce the Paris Law response experimentally observed in delamination growth in

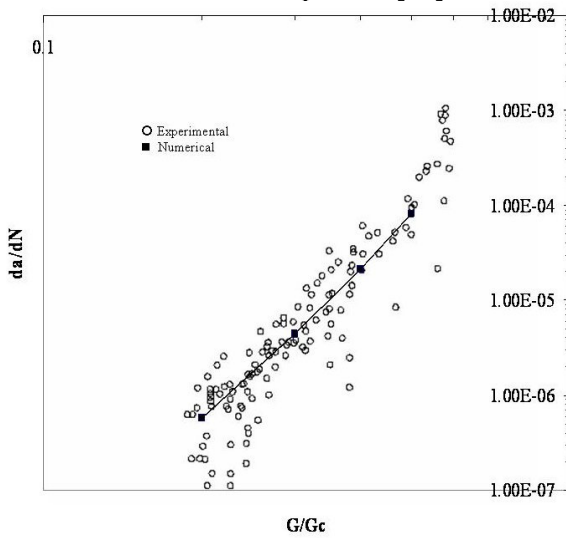polymer matrix composites. The experimental data comes from the work of Asp et al. [12]



Fig. 10. Paris plot with experimental and numerical results

## 4.2 Influence of Δl and ΔN

Using the bilinear interface law, the slope ($da/dN$) computed for very small values of $\Delta N$ and $\Delta l$ ($\Delta N$ =100 cycles , $\Delta l$ =0.005 mm.) was used as a baseline, it is called the 'exact solution'. After a large number of results with different values of $\Delta N$ and $\Delta l$ were obtained, they were compared against the 'exact solution' and divided into ranges depending on the variation shown.

In order to produce Figure 11, $\Delta N$ and $\Delta l$ were normalised by dividing them by the number of cycles required to break a spring ($N_a$) and the length of the active zone ($l_a$) respectively. The inverse of the ratio $\Delta N/N_a$ is related to the number of increments needed to completely break the length of the active zone while the inverse of $\Delta l/l_a$ provides the number of elements in the active zone.

There are some interesting features that can be observed in Figure 11. The first one is the formation of vertical bands that change abruptly for small changes in values of $\Delta N/N_a$. These bands go from 'good' values of the slope, on the left, to 'bad' ones on the right, in which the slope computed is significantly different to the exact solution.

The second feature that can be observed is the formation on the left side of the chart of some peaks of 'bad' results that blend into 'better' results as they move to the right of the chart. As opposed to the vertical bands, these computed results are for values of the slope that are larger than the baseline.
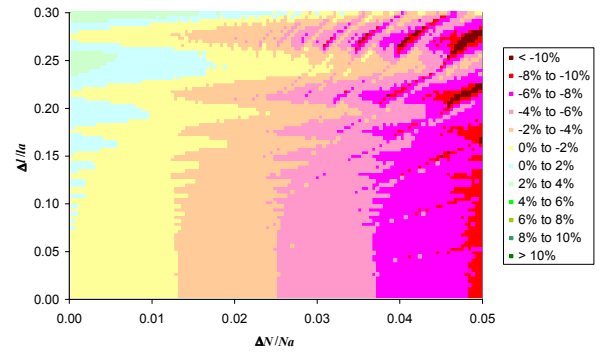


Fig. 11. Influence of $\Delta l$ and $\Delta N$ using the bilinear interface law with the stiffness degradation based damage formulation
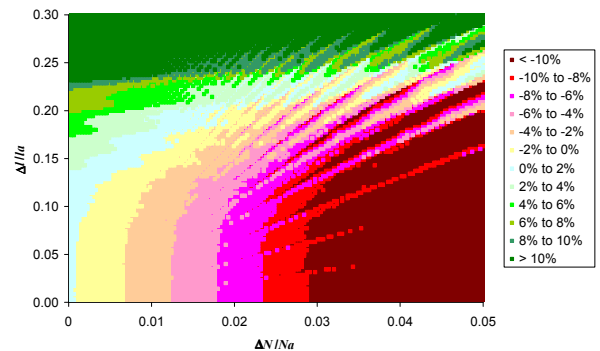


Fig 12. Influence of $\Delta l$ and $\Delta N$ using the polynomial interface law with the stiffness degradation based damage formulation
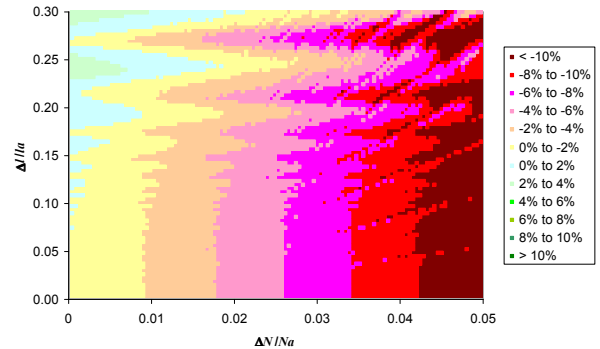


Fig. 13. Influence of $\Delta l$ and $\Delta N$ using the bilinear interface law with the area based damage formulation
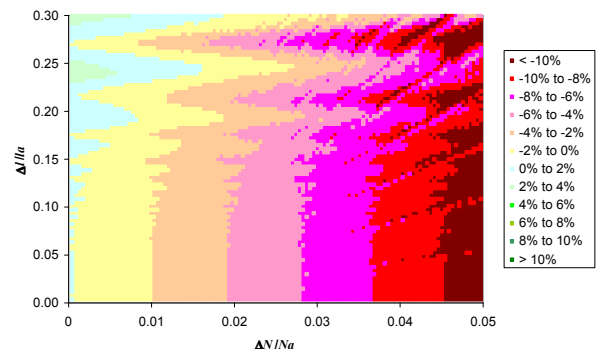


Fig. 14 Influence of $\Delta l$ and $\Delta N$ using the bilinear interface law with the energy based damage formulation

It can also be seen that the central part of these peaks correspond to the results where there is an integer number of elements in the active zone. For example, the large peak located at $\Delta l / l_a$=0.25 corresponds to 4 active elements. Moving downwards it can be seen that the next peak coincides with $\Delta l / l_a$=0.20 which corresponds to 5 active elements and so on.

An analysis was performed to understand the formation of these peaks and it showed that the number of elements in the active zone, a direct result of the value of $\Delta l$ chosen, has an influence in the accuracy of the results obtained. It can be inferred from this analysis that in order to have reasonable results the model should have at least 5 elements in the active zone.

The third feature that can be observed is the pattern of some radial lines that seem to come from the origin. These lines are made of 'better' results that are embedded in zones with 'worse' ones. It should be highlighted that the slopes of these lines seem to roughly correspond to integer values, e.g. 1, 2, 3, etc. Also these lines blur into the peaks mentioned in the previous paragraph leaving us with zones of 'good' results being surrounded by 'bad' results.

An analysis was made in order to understand the formation of the radial lines and it seems that a number of combinations for $\Delta N$ and $\Delta l$ are able to provide good results when they are not supposed to do so and it was concluded that this phenomenon occurred due to the way the problem is being modelled.

The polynomial interface law coupled with the bilinear interface constitutive law was also used to study the influence of $\Delta l$ and $\Delta N$ in the model. The results are shown in Figure 12.

The first feature to be noticed is that the vertical bands related to the variations of $\Delta N / N_a$ are compacted in respect to Figure 11 and this shows an increased sensitivity to variations in the values of $\Delta N$.

The second feature that can be observed in Figure 12 is that there is also an increased sensitivity to variations in the values of $\Delta l$. This means than more elements are required in the active zone in order to provide reliable results.

The presence of the radial lines whose slope values correspond to integers is very clear in Figure 12 as well as the presence of 'good' results embedded in 'bad' results zones.

Something that should be mentioned is that the values of the coefficients $\beta$ and $C$ varied greatly than

with those used in the bilinear interface law as it can be seen in Table 2.

It also must be mentioned that the length of the active zone using this interface constitutive law was significantly larger than the values obtained for the bilinear interface law using the three different damage formulations as it can be seen in Table 3.

| | $l_a$ | |
|---|---|---|
| Bilinear law, stiffness | 0.6675 | mm. |
| Polynomial law, stiffness | 0.8750 | mm. |
| Bilinear law, area | 0.6625 | mm. |
| Bilinear law, energy | 0.6650 | mm. |

Table 3. Length of the active zone ($l_a$) for the different formulations that were tested.

The influence of $\Delta l$ and $\Delta N$ using the two energy based damage formulations coupled with the bilinear interface constitutive law were also explored.

In Figure 13 the influence of $\Delta l$ and $\Delta N$ under the first energy based damage formulation along with the bilinear interface law is shown. It can be observed that the same features of Figure 11, such as the vertical bands, peaks and radial lines, are present but with a relative increased sensitivity to the number of cycles ($\Delta N$) applied for every load step.

For this formulation a large difference in the value of the coefficient $C$ compared with the stiffness based one was found as well as a smaller difference for coefficient $\beta$ as shown in Table 2.

The length of the active zone for this damage formulation was very similar to the stiffness degradation based formulation as it can be seen in Table 3.

The influence of $\Delta l$ and $\Delta N$ using the second energy based damage formulation combined with the bilinear interface law can be seen in Figure 14. It can be appreciated that all of the features previously discussed (vertical bands, peaks and radial lines) are present and that this figure is almost identical to Figure 13 and very similar to Figure 11.

The values of the coefficients $\beta$ and $C$ used for this damage formulation were in the same order of magnitude than the ones used in the previous formulation as shown in Table 2.

The length of the active zone for the second energy based damage formulation is very similar to the one of the other two formulations involving the bilinear interface law as shown in Table 3.

## Conclusions

A simple model that represents interface elements subjected to fatigue loading has been developed and validated.

Three different constitutive laws for interface elements have been implemented in the model and analysed: bilinear, third-order polynomial and linear-polynomial with a stiffness degradation based damage formulation. Also, two additional static damage formulations based on energy have been proposed and developed into fatigue loading ones.

A study of the influence of $\Delta l$ and $\Delta N$ showed that the various interface laws and damage formulations exhibit a very similar pattern to that shown in Figure 11. The figure confirms that the more accurate results are found for smaller values of $\Delta l$ and $\Delta N$. Figures like this are currently being used to identify the combination of interface element formulation/fatigue damage degradation that is least sensitive to the values selected for $\Delta l$ and $\Delta N$.

The bilinear interface constitutive law coupled with the stiffness degradation based damage formulation has proved to be the least sensitive to variations in the values of $\Delta l$ and $\Delta N$.

The polynomial interface constitutive law has been found to be the most sensitive to changes in the values of $\Delta l$ and $\Delta N$. The length of the active zone ($l_a$) for this interface law was considerably larger than when using the bilinear one. Also, the values of the coefficients $\beta$ and $C$ for this law were significantly different than the other ones.

The two energy based damage formulations, coupled with the bilinear interface constitutive law, are similar to each other in the sensitivity to variations in the values of $\Delta l$ and $\Delta N$, the values of the coefficients $\beta$ and $C$ required and in the length of the active zone, which is very similar to the value obtained when using the stiffness degradation based damage formulation and the bilinear interface constitutive law.

## Acknowledgements

## References

[1] Van Paepegem, W., Degrieck, J. and De Baets, P., Finite element approach for modelling fatigue damage in fibre-reinforced composite materials. *Composites Part B: Engineering*, Vol. 32, pp 575-588, 2001.

[2] Siegmund, T. A numerical study of transient fatigue crack growth by use of an irreversible cohesive zone model. *International Journal of Fatigue*, Vol. 26, pp 929-939, 2004.

[3] Turon, A., Camanho, P.P., Costa, J. and Dávila, C.G., A damage model for the simulation of delamination in advanced composites under variable-mode loading. *Mechanics of Materials*, Vol. 38, No. 11, pp 1072-1089, 2006.

[4] Turón, A., *Simulation of delamination in composites under quasi-static and fatigue loading using cohesive zone models*, Ph.D. Thesis, Universitat de Girona: Girona, Spain, 2006.

[5] Allix, O., Ladevéze, P. and Corigliano, A., Damage analysis of interlaminar fracture specimens. *Composite Structures*, Vol. 31, pp 61-74, 1995.

[6] Alfano, G. and Crisfield, M.A., Finite element interface models for the delamination analysis of laminated composites: mechanical and computational issues. *International Journal for Numerical Methods in Engineering*, Vol. 50, No. 7, pp 1701-1736, 2001.

[7] Robinson, P., Galvanetto, U., Tumino, D. and Belluci, G., Numerical simulation of fatigue-driven delamination using interface elements. *International Journal for Numerical Methods in Engineering*, Vol. 63, No. 13, pp 1824-1848, 2005.

[8] Muñoz, J.J., Galvanetto, U. and Robinson, P., On the numerical simulation of fatigue driven delamination with interface elements. *International Journal of Fatigue*, Vol. 28, No. 10, pp 1136-1146, 2006.

[9] Tvergaard, V. Effect of fibre debonding in a whisker-reinforced metal. *Materials Science and Engineering A*, Vol. 125, pp 203-213, 1990.

[10] Pinho, S.T., Ianucci, L. and Robinson, P., Formulation and implementation of decohesion elements in an explicit finite element code. *Composites Part A: Applied Science and Manufacturing*, Vol. 37, No. 5, pp 778-789, 2006.

[11] Peerlings, R.H.J., Brekelmans, W.A.M., de Borst, R. and Geers, M.G.D., Gradient-enhanced damage modelling of high-cycle fatigue. *International Journal for Numerical Methods in Engineering*, Vol. 49, No. 12, pp 1547-1569, 2000.

[12] Asp, L.E., Sjörgen, A. and Greenhalgh, E.S., Delamination growth and thresholds in a carbon/epoxy composite under fatigue loading. *Journal of Composites Technology and Research*, Vol. 23, pp 55-68, 2001.